A Mutational Analysis of the Binding of Two Different Proteins to the Same Antibody†

William Dall'Acqua,‡ Ellen R. Goldman,‡ Edward Eisenstein,‡,§ and Roy A. Mariuzza*,‡

Center for Advanced Research in Biotechnology, University of Maryland Biotechnology Institute, 9600 Gudelsky Drive, Rockville, Maryland 20850, and Department of Chemistry and Biochemistry, University of Maryland Baltimore County, Baltimore, Maryland 21228

Received April 5, 1996⊗

ABSTRACT: The crystal structures of the complexes between the anti-hen egg white lysozyme (HEL) antibody D1.3 and HEL and between D1.3 and the anti-D1.3 antibody E5.2 have shown that D1.3 contacts these two proteins through essentially the same set of combining site residues [Fields, B. A., Goldbaum, F. A., Ysern, X., Poljak, R. J., & Mariuzza, R. A. (1995) *Nature 374*, 739−742]. To probe the relative contribution of individual residues to complex stabilization, single alanine substitutions were introduced in the combining site of D1.3, and their effects on affinity for HEL and for E5.2 were measured using surface plasmon resonance detection, fluorescence quench titration, or sedimentation equilibrium. The energetics of the binding to HEL are dominated by only 3 of the 13 contact residues tested ($\Delta G_{mutant} - \Delta G_{wild\ type} > 2.5$ kcal/mol): V_LW92, V_HD100, and V_HY101. These form a patch at the center of the interface and are surrounded by residues whose apparent contributions are much less pronounced (<1.5 kcal/mol). This contrasts with the interaction of D1.3 with E5.2 in which most the contact residues (11 of 15) were found to play a significant role in ligand binding (>1.5 kcal/mol). Furthermore, even though D1.3 contacts HEL and E5.2 in very similar ways, the functionally important residues of D1.3 are different for the two interactions, with only substitutions at D1.3 positions V_H100 and V_H101 greatly affecting binding to both ligands. Thus, the same protein may recognize different ligands in ways that are structurally similar yet energetically distinct.

The three-dimensional structures of a number of antigen−antibody complexes have been determined in recent years (Davies *et al*., 1990; Mariuzza & Poljak, 1993; Webster *et al*., 1994; Braden & Poljak, 1995). These studies have permitted a detailed description of antigenic determinants and of antibody combining sites. They have also provided important information on the general characteristics of protein−protein complexes, such as the size and chemical nature of the interfaces and the magnitude of conformational changes associated with complex formation (Janin & Chothia, 1990; Wilson & Stanfield, 1993; Davies & Cohen, 1996). However, the relative contributions of hydrophobicity, surface complementarity, and hydrogen bonding to the energetics of binding, the role of bound water molecules in complex stabilization (Kornblatt *et al*., 1993; Bhat *et al*., 1994; Goldbaum *et al*., 1996), and the mechanisms by which amino acid changes in the interface are accommodated (Tulip *et al*., 1992; Ysern *et al*., 1994) remain to be clarified. Another important issue is whether productive binding is mediated by a small subset of interface residues (Novotny *et al*., 1989; Cunningham & Wells, 1993; Kelley & O'Connell, 1993; Tulip *et al*., 1994) or whether complex cooperative interactions involving most of the contacting residues are responsible for the observed affinities. Clackson and Wells (1995) addressed this question in the case of the interaction of human growth hormone with its receptor. These authors replaced contact residues in the receptor and showed that binding to growth hormone is generated through a few strong interactions. This so-called "functional epitope" forms a central hydrophobic region, dominated by two tryptophan residues, that seems to account for most of the binding free energy. The same trend was found by Cunningham and Wells (1993), who analyzed the hormone side of the interface and found that only 8 out of 31 side chains appeared to contribute significantly to productive binding. However, the extent to which these results are general ones remains to be established.

To address this issue, we have studied the binding of the monoclonal antibody D1.3 to two structurally distinct ligands: its cognate antigen, hen egg white lysozyme (HEL),[1] and the anti-idiotypic antibody E5.2. The crystal structure of the complex formed by the Fv fragment (a heterodimer consisting of only the light and heavy chain variable domains, V_L and V_H) of D1.3 with HEL has been determined to a nominal resolution of 1.8 Å (Bhat *et al*., 1994). In addition, the structure of the complex between the Fv fragments of D1.3 and the anti-D1.3 antibody E5.2 is known to 1.9 Å resolution (Fields *et al*., 1995). Surprisingly, it was found that D1.3 contacts HEL and E5.2 through essentially the same set of combining site residues (and most of the same

† This work was supported by NIH Grants GM52801 (R.A.M.) and RR08937 (E.E.).

* Author to whom correspondence should be addressed. Tel.: 301-738-6243. FAX: 301-738-6255. E-mail: mariuzza@indigo2.carb.nist.gov.

‡ University of Maryland Biotechnology Institute.

§ University of Maryland Baltimore County.

⊗ Abstract published in *Advance ACS Abstracts,* July 1, 1996.

[1] Abbreviations: HEL, hen egg white lysozyme; scFv, single chain Fv fragment; PBS, phosphate-buffered saline; Ni^{2+}-NTA, nickel nitriloacetic acid; IPTG, isopropyl β-D-thiogalactoside; PCR, polymerase chain reaction; HBS, Hepes-buffered saline; RU, resonance units; CDR, complementarity-determining region; V_L, light chain variable region; V_H, heavy chain variable region.

S0006-2960(96)00819-7 CCC: $12.00

atoms). In addition, the positions of the atoms of E5.2 that contact D1.3 are close to those of HEL that contact D1.3, and 6 of the 12 interface hydrogen bonds in the D1.3−E5.2 complex are structurally equivalent to hydrogen bonds in the D1.3−HEL interface. Thus, E5.2 mimics HEL in its binding interactions with D1.3. Confirming these observations, E5.2 induces an anti-HEL response when used as an immunogen (Fields *et al*., 1995). Because D1.3 recognizes HEL and E5.2 through structurally similar interactions, this constitutes an excellent model for determining whether the same antibody combining site binds two different ligands in energetically similar ways.

The apparent contribution of individual residues of the Fv fragment of D1.3 to binding HEL and FvE5.2 was determined by comparing the binding of wild-type protein with that of mutants in which the side chains were truncated by site-directed mutagenesis (Fersht, 1988). Alanine-scanning mutagenesis (Wells, 1991) was carried out on all residues of D1.3 in contact with HEL and/or E5.2. Alanine was chosen because it eliminates the side chain without altering the main-chain conformation and does not impose extreme steric or electrostatic effects. Affinities were measured using three independent techniques (surface plasmon resonance detection, fluorescence quench titration, and sedimentation equilibrium) in order to assure the accuracy of our results. We show that the functionally important residues of D1.3 are different for binding HEL and E5.2. We also find that while the D1.3−HEL interaction is dominated by a small subset of contact residues, as described for the binding of growth hormone to its receptor (Cunningham & Wells, 1993; Clackson & Wells, 1995), a much larger subset contributes to the D1.3−E5.2 reaction. Thus, the notion that protein−protein recognition is mediated by only a few strong interactions (Novotny *et al*., 1989; Cunningham & Wells, 1993; Kelley & O'Connell, 1993; Tulip *et al*., 1994; Clackson & Wells, 1995) may not be a general one. In certain cases, the free energy of binding may arise from the accumulation of many interactions of varying strength over the entire protein−protein interface.

MATERIALS AND METHODS

Reagents. All chemicals were of analytical grade. Restriction enzymes and DNA-modifying enzymes were purchased from New England Biolabs, Inc. (Beverly, MA). Radiolabeled [^{35}S]dATP was obtained from Amersham Corp. Oligonucleotides were synthesized on a 380B DNA synthesizer (Applied Biosystems, Foster City, CA).

Production of Fv Fragments. The monoclonal anti-HEL antibody D1.3 is derived from a Balb/c mouse hyperimmunized with this antigen (Mariuzza *et al*., 1984). The single chain version of FvD1.3 (scFvD1.3; McCafferty *et al*., 1990) and of the mutants was prepared from the culture supernatant of recombinant *Escherichia coli* BMH 71−18 cells (Ruther *et al*., 1981) transformed with the pUC19-based dicistronic expression vector pSW1 (Ward *et al*., 1989). The single chain linker, $(Gly_4Ser)_3$, is identical to that used previously for immunoglobulin scFvs by Huston *et al*. (1988). For protein production, recombinant clones were resuspended in 10 mL of 4×YT medium (double strength 2×YT) containing 100 μg/mL ampicillin and 1% (w/v) glucose. The presence of glucose is necessary for normal growth of recombinant *E. coli* cells; it represses scFvD1.3 gene expression, whose production is toxic to the cells. The cultures were incubated at 37 °C under agitation to an absorbance of 1.0 at 600 nm. The cells were then pelleted by centrifugation, washed twice with 4×YT, and resuspended in 500 mL of 4×YT containing 100 μg/mL ampicillin and 0.1% (w/v) glucose. This glucose concentration is high enough for cells to grow normally, yet low enough to permit efficient induction following its depletion from the medium as a result of metabolism by *E. coli*. The cultures were grown at 30 °C to an absorbance of 1.0, and isopropyl β-D-thiogalactoside (IPTG; Gold Biotechnology, St. Louis, MO) was added to a final concentration of 0.2 mM. After further incubation at 30 °C for 18 h, the bacteria were pelleted, and scFvD1.3 was affinity purified from the supernatant using monoclonal antibody E5.2− (Goldbaum *et al*., 1994) or HEL− (Ysern *et al*., 1994) Sepharose columns. Columns were washed with 10 volumes of phosphate-buffered saline (PBS), pH 7.4, and eluted with 50 mM diethylamine, pH 12. Fractions were immediately neutralized with 1.0 M Tris-HCl, pH 7.0.

The V_L and V_H genes of monoclonal antibody E5.2 were cloned from the corresponding hybridoma cell line as described (Goldbaum *et al*., 1994). The amplified genes were then inserted into the pUC19-based dicistronic expression vector pSW1 (Ward *et al*., 1989) as an *Eco*RI/*Hin*dIII fragment, such that each gene is fused in-frame with the signal sequence of pectate lyase in order to direct secretion of the V domains into the periplasmic space of *E. coli*. A His_6 tail was grafted onto the 3′ end of the V_L gene of FvE5.2 by means of the polymerase chain reaction (PCR) to permit affinity purification using a nickel chelate adsorbent (Hochuli *et al*., 1988). The amplification mixture included 100 ng of pSW1-E5.2 DNA, 50 pmol of each of the primers 5′-AGTGCCAAGCTTGCATGCAAA-3′ (*Hin*dIII site underlined) and 5′-GATTACGAATTCGAGCTGGATCCTTATT-AGTGATGGTGATGGTGATGGGTGACCGGTTTGAT-CTCCAG-3′ (*Eco*RI site underlined), 200 μM each dNTP, 100 mM Tris-HCl, pH 8.3, 500 mM KCl, 1.5 mM $MgCl_2$, 0.01% (w/v) gelatin, and 2.5 units of AmpliTaq polymerase (Perkin Elmer). The sample was overlaid with paraffin oil, heated to 94 °C for 5 min, and subjected to a further 25 rounds of temperature cycling (94 °C for 1 min, 50 °C for 1 min, and 72 °C for 1 min) using an Eppendorf MicroCycler E programmable heating block. The amplified DNA was digested with *Eco*RI and *Hin*dIII and cloned into the pSW1 expression vector restricted with the same enzymes.

For production of FvE5.2, recombinant BMH 71−18 *E. coli* cells were grown at 37 °C in 10 mL of 4×YT containing 100 μg/mL ampicillin and 1% glucose (w/v) to an absorbance at 600 nm of 1.0. Three milliliters of this preculture was used to inoculate 500 mL of 4×YT containing 100 μg/mL ampicillin and 0.1% glucose (w/v). After growth at 30 °C to an absorbance of 1.0, the bacteria were induced with 0.1 mM IPTG and incubated an additional 5 h at this temperature. The recombinant protein was located in the periplasm and could be isolated by osmotically shocking the cells as described (Ward, 1992). The osmotic shock fraction (75 mL for 1 L of culture) was extensively dialyzed against PBS and applied to a 1 mL nickel nitrilotriacetic acid (Ni^{2+}-NTA) affinity column (QIAGEN). The column was washed with 20 volumes of 500 mM NaCl and 100 mM Tris-HCl, pH 8.0. The Fv fragment was eluted in 5 mL of 300 mM imidazole, pH 7.5. The protein was then dialyzed against PBS containing 1 mM EDTA.

Further purification of both scFvD1.3 and FvE5.2 was carried out by size exclusion chromatography on a ZORBAX GF-250 column (Dupont) in 0.2 M sodium phosphate buffer, pH 7.4, where they eluted as single peaks of approximately 25 kDa. Final yields were typically 0.5−1.0 mg/L of culture.

Site-Directed Mutagenesis. Mutagenesis of scFvD13 (McCafferty *et al*., 1990) was carried out after subcloning of the gene as an *Hin*dIII/*Eco*RI fragment into M13mp18 as described (Kunkel *et al*., 1987) with a Muta-Gene M13 *in vitro* mutagenesis kit (Bio-Rad, Richmond, CA). The mutagenic oligonucleotides were designed to replace the wild-type codons with that for alanine (GCT). Prior to expression, all mutations were confirmed by the dideoxynucleotide sequencing method (Sanger, 1977) using a Sequenase Version 2.0 kit (USB, Cleveland, OH).

BIAcore Analysis of HEL−scFvD1.3 and FvE5.2−scFvD1.3 Interactions. The interaction of soluble scFvD1.3 with immobilized HEL was monitored by surface plasmon resonance detection using a BIAcore instrument (Pharmacia Biosensor, Uppsala, Sweden). All proteins were purified by gel filtration prior to use as described above in order to eliminate aggregated material which could interfere with affinity measurements (van der Merwe *et al*., 1993, 1994). Protein concentrations were calculated using 1% extinction coefficients at 280 nm of 1.50 for both scFvD1.3 and FvE5.2 and 2.62 for HEL. The latter was coupled to the dextran matrix of a CM5 sensor chip (Pharmacia Biosensor) using an Amine Coupling Kit as described (Johnsson *et al*., 1991). Lysozyme, whose isoelectric point is above 10, was dialyzed against 10 mM sodium acetate, pH 5.0. The protein concentration ranged from 25 to 100 μg/mL. The activation and immobilization periods were both set to between 3 and 7 min at a flow rate of 5 μL/min. Excess reactive esters were quenched by injection of 35 μL of 1.0 M ethanolamine hydrochloride, pH 8.5. Typically, between 200 and 1500 resonance units (RU) of HEL was immobilized under these conditions. Single chain FvD1.3 and the mutants were dialyzed against Hepes-buffered saline (HBS) containing 150 mM NaCl, 0.005% Surfactant P-20 (Pharmacia), and 10 mM Hepes, pH 7.5; dilutions were made in the same buffer. All binding experiments were performed at 25 °C. Pulses of 10 mM HCl were used to regenerate the surfaces.

Runs were analyzed using the software BIAevaluation 2.1 (Pharmacia). Association constants (K_As) were determined from Scatchard analysis by measuring the concentration of free reactants and complex at equilibrium. In equilibrium binding BIAcore experiments (Karlsson *et al*., 1991; van der Merwe *et al*., 1993, 1994; Raghavan *et al*., 1994; Malchiodi *et al*., 1995), the concentration of the complex can be assessed directly as the steady-state response. The concentration of free analyte (scFvD1.3 or FvE5.2) is equal to the bulk analyte concentration since analyte is constantly replenished during sample injection. The concentration of free ligand on the surface of the sensor chip can be derived from the concentration of the complex and from the total binding capacity of the surface as

$$K_A = R_{eq}/C(R_{max} - R_{eq})$$

where C is the free analyte concentration, R_{eq} is the steady-state response, and R_{max} is the total surface binding capacity. Rearranging, we obtain

$$R_{eq}/C = K_A R_{max} - K_A R_{eq}$$

A plot of R_{eq}/C versus R_{eq} at different analyte concentrations thus gives a straight line from which K_A can be calculated; R_{max} is derived from the intercept on the x-axis. Standard deviations for two or more independent determinations were <30%.

Measurements of the binding of FvE5.2 to scFvD1.3 were carried out essentially as described above except that streptavidin was immobilized to capture biotinylated scFvD1.3. Briefly, streptavidin (Sigma) at 200 μg/mL in 10 mM sodium acetate, pH 4.5, was coupled to the sensor chip under the same conditions as described above for HEL. Biotinylation of scFvD1.3 was performed using an Immunoprobe biotinylation kiet (Sigma). Binding of biotinylated scFvD1.3 to immobilized streptavidin was carried out at pH 7.2 at concentrations ranging from 50 to 100 μg/mL in PBS at a flow rate of 5 μL/min; this typically resulted in the immobilization of between 200 and 500 RU. Association constants for the binding of FvE5.2 to scFvD1.3 were determined by Scatchard analysis as for the binding of scFvD1.3 to HEL.

Fluorescence Measurements. Fluorescence emission spectra showed quenching of tryptophan fluorescence on formation of a complex of scFvD1.3 (wild type or mutant) with FvE5.2. Measurements were performed at 25 °C in HBS containing 0.005% Surfactant P-20 on a SPEX FloroMAX spectrofluorometer (SPEX Industries, Edison, NJ) run by SPEX DM3000 software and equipped with a temperature controller and magnetic stirrer. Affinity constants were determined by titrating D1.3 with E5.2 and monitoring the fluorescence at a single wavelength (Ward, 1985; Foote & Winter, 1992). An excitation wavelength of 290 nm (1 nm slit) was used; fluorescence emission was recorded at 390 nm (5 nm slit). This wavelength was chosen as opposed to the fluorescence maximum of the D1.3 emission spectra, or the fluorescence difference spectra, as the fractional quench at 390 nm was at least 15% for all the mutants tested.

Fluorescence emission was measured for a 3 mL sample of antibody (20−100 nM). In a typical titration, aliquots of concentrated FvE5.2 stock were added to final concentrations of 5, 10, 20, 40, 80, 160, and 320 nM. Data were collected over 2 min, and 10 min was allowed between the addition of FvE5.2 and fluorescence measurement. The fluorescence emission for a blank titration of FvE5.2 to the same final concentrations was also collected. The E5.2 titration gave a linear increase in fluorescence over the whole concentration range, while the D1.3 titrations with E5.2 showed an initial decrease in fluorescence before a linear rise. The surfactant in HBS prevented the loss of fluorescence due to adsorption to the glass.

The data were processed on a Macintosh running KaleidaGraph. For each concentration of E5.2, a value F was calculated according to

$$F = (\text{fluorescence measured} - \text{fluorescence of D1.3 alone}) - \text{fluorescence of E5.2}$$

and a plot of F versus concentration of E5.2 was constructed.

The resulting curve was fitted to the equation:

$$F = (0.5)(V)([D1.3] + [E5.2] + (1/K_A) - (([D1.3] + [E5.2] + (1/K_A))^2 - 4[E5.2][D1.3])^{1/2})$$

where V is the molar fluorescence change occurring on the binding of D1.3 and E5.2 and K_A is the association constant.

Sedimentation Equilibrium. Equilibrium sedimentation experiments were performed on a Beckman XL-A Optima analytical ultracentrifuge using a four-hole An-55 rotor at 25 °C and a rotor speed of 28 000 rpm. Data were acquired as an average of 25 measurements of absorbance at each radial position, with a nominal spacing of 0.001 cm between radial positions. Samples were prepared in PBS. A molar extinction coefficient of 36 000 M^{-1} cm^{-1} was used for both scFvD1.3 and FvE5.2. Partial specific volumes were assumed to be 0.73 mL/mg, and solvent densities were determined pychnometrically. Equilibrium sedimentation data on the individual scFvD1.3 and FvE5.2 species obtained at either two different rotor speeds or two initial protein concentrations were analyzed for average molecular weights in terms of a single, homogeneous species according to

$$c_r = B + c_m \exp[M(1 - \nu\rho)\omega^2(r^2 - r_m^2)/2RT]$$

where c_r is the concentration of the protein at a given radial position, c_m is the concentration of the protein at some reference position (*e.g.*, the meniscus), M is the molecular weight, ν is the partial specific volume, ρ is the solvent density, ω is the angular velocity, r is the radial position in centimeters from the center of rotation, r_m is the distance in centimeters from the center of rotation to the meniscus, R is the gas constant, T is the absolute (Kelvin) temperature, and B is a correction term for a nonzero baseline.

Equilibrium constants for the association of FvE5.2 and the scFvD1.3 V_HW52A mutant were calculated from the data obtained at sedimentation equilibrium according to

$$c_r = B + c_{m,D} \exp[M_D(1 - \nu r)\omega^2(r^2 - r_m^2)/2RT] + (c_{m,E}) \exp[M_E(1 - \nu r)\omega^2(r^2 - r_m^2)/2RT] + (c_{m,D})(c_{m,E})/(1/K_A) \exp[M_C(1 - \nu\rho)\omega^2(r^2 - r_m^2)/2RT]$$

where $c_{m,D}$ is the concentration of scFvD1.3 at the reference position, $c_{m,E}$ is the concentration of FvE5.2 at the reference position, M_D and M_E are the molecular weights of the scFvD1.3 and FvE5.2 as determined in separate sedimentation equilibrium experiments, M_C is the molecular weight of the complex, and K_A is the association constant for the scFvD1.3−FvE5.2 interaction. Parameters were evaluated using nonlinear least-squares analysis (Johnson *et al.*, 1981) or by using a modified version of IGOR (Wavemetrics, Lake Oswego, OR) running on a Macintosh computer (Brooks *et al.*, 1993, 1994). Data for two different concentrations or two rotor speeds were analyzed simultaneously as a test for homogeneity and reversibility (Roark, 1976) and to constrain confidence intervals for the parameter values (Johnson & Fraser, 1985). Errors on K_As were about 20% of parameter values.

RESULTS AND DISCUSSION

Determination of Equilibrium Constants for the Binding of scFvD1.3 to HEL and FvE5.2 by Surface Plasmon Resonance Detection. For all BIAcore experiments, FvE5.2, scFvD1.3, and mutants of scFvD1.3 were purified to >90% homogeneity, as judged by SDS−PAGE (Figure 1); scFvD1.3 migrated as a single species of about 30 kDa, while FvE5.2 migrated as two closely spaced bands of approximately 15 kDa, corresponding to the V_H and V_L polypeptide chains. In order to analyze the interaction of mutants of scFvD1.3 with HEL, the latter was coupled directly to the dextran matrix through primary amine groups of the protein. Injection of different concentrations of scFvD1.3 over the immobilized ligand gave concentration-dependent binding. Typical surface plasmon resonance profiles for equilibrium binding of wild-type scFvD1.3 and the mutant V_LH30A to HEL are shown in Figure 2 (panels A and B). To estimate apparent K_As, concentrations of scFvD1.3 ranging from 5 nM to 20 μM were used, depending on the affinity of the particular mutant: higher concentrations of scFvD1.3 were required to approach saturation for low-affinity mutants. In all cases, equilibrium binding levels were reached within 7 min. To estimate the increase in RU resulting from the nonspecific effect of protein on the bulk refractive index, binding of scFvD1.3 to a control surface with no immobilized ligand was also measured (data not shown). Typically, this nonspecific signal was not significant for analyte concentrations up to 1 μM. The Scatchard plots for the binding of wild-type scFvD1.3 and the V_LH30A mutant, after correction for nonspecific binding, are shown in Figure 2 (panels C and D). The plots were linear, and apparent K_As were calculated as the slopes of the straight lines. Following the last injection of scFvD1.3, the analyte was reinjected at one of the initial concentrations to determine whether HEL on the dextran matrix had undergone significant denaturation as the result of repeated regenerations of the surface with 10 mM HCl. Very similar signals were obtained even following 15 regenerations, indicating that the immobilized ligand effectively retained its original binding activity. The predicted maximum specific binding, calculated from the *x*-intercept assuming a linear relationship between the mass of bound protein and the measured RU (Granzow *et al.*, 1992), indicated that at least 85% of the HEL molecules on the chip were available for binding.

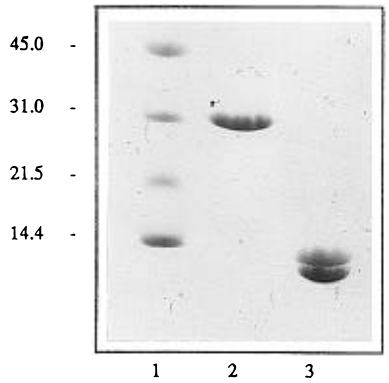

FIGURE 1: SDS−PAGE profile of purified wild-type scFvD1.3 and FvE5.2. Samples were run in PhastGel Homogeneous 20 gels. Lane 1, molecular mass standards (Bio-Rad) ovalbumin (45.0 kDa), carbonic anhydrase (31.0 kDa), trypsin inhibitor (21.5 kDa), and lysozyme (14.4 kDa); lane 2, scFvD1.3; lane 3; FvE5.2.

Efforts to examine binding in the reverse orientation (*i.e.*, with scFvD1.3 on the sensor surface and HEL in solution) were not successful. Although specific binding was detected, the weak and nonreproducible response upon injection of HEL precluded quantitative analysis. Similar difficulties

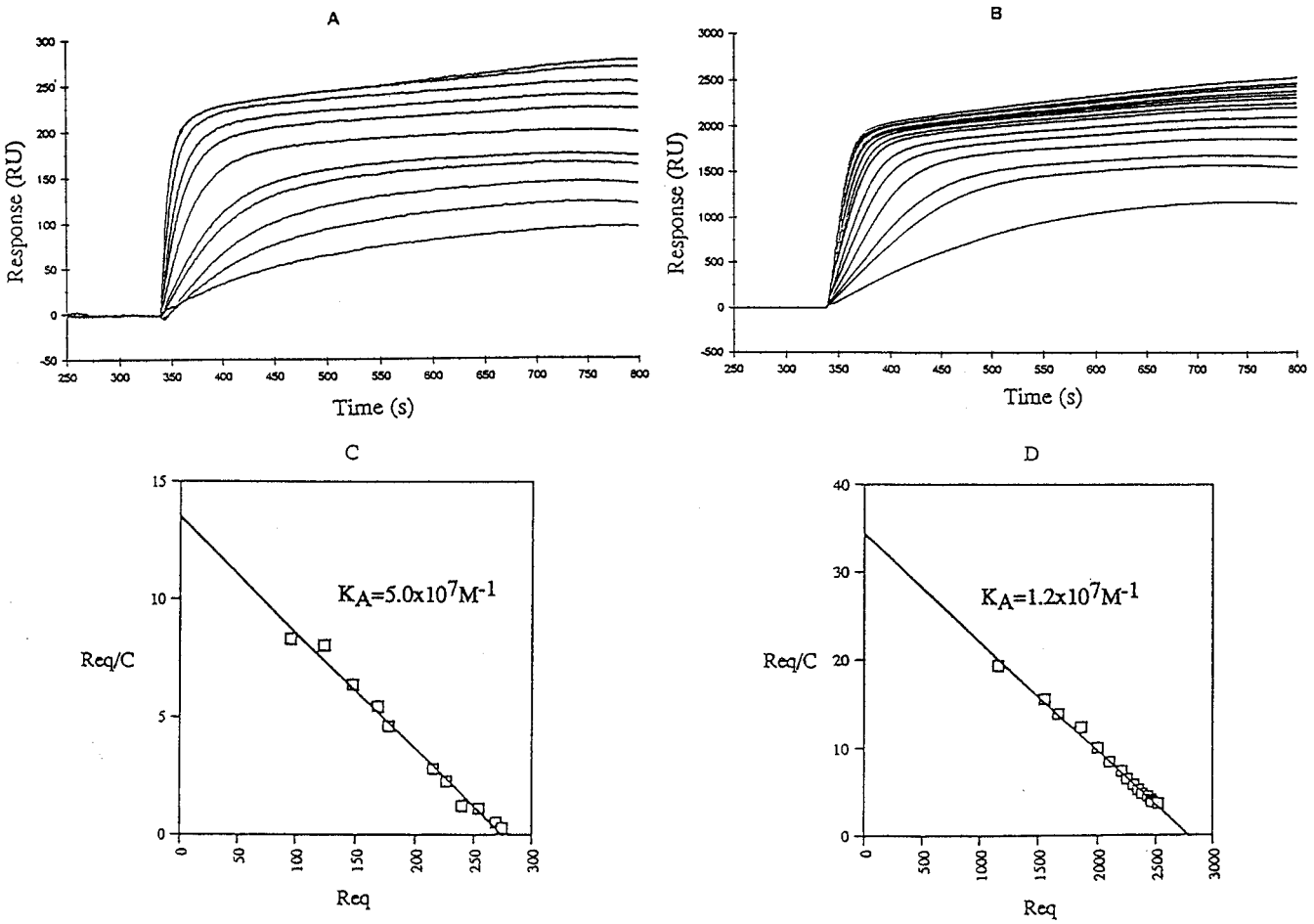

FIGURE 2: (A) Binding of wild-type scFvD1.3 to immobilized HEL. Wild-type scFvD1.3 was injected at 11 different concentrations ranging from 10 nM to 1 μM over a surface to which 120 RU of HEL had been coupled. Buffer flow rates were 5 μL/min. Equilibrium binding levels were reached within 7 min. After equilibrium was reached, residual bound protein was eluted using a 1 min pulse of 10 mM HCl. (B) Binding of the V_LH30A scFvD1.3 mutant to immobilized HEL. The mutant was injected at 15 different concentrations of V_LH30A ranging from 60 nM to 0.7 μM over a surface to which 1200 RU of HEL had been coupled. (C and D) Scatchard analysis of the binding of wild-type scFvD1.3 and V_LH30A to HEL. Plots are from the data in (A) and (B), respectively, after correction for nonspecific binding (see Materials and Methods); Req is the corrected equilibrium response at a given concentration *C*. The plots are linear with correlation coefficients of 0.994 and 0.997, respectively. The apparent K_A for the wild-type scFvD1.3−HEL interaction is 5.0×10^7 M^{-1} and for the V_LH30A−HEL interaction 1.2×10^7 M^{-1}.

have been reported for the binding of bacterial superantigens to immobilized T-cell receptors (Seth *et al*., 1994; Malchiodi *et al*., 1995). This prompted us to confirm our BIAcore measurements by sedimentation equilibrium and fluorescence quench titration (see below), techniques which do not require ligand immobilization.

The interaction of scFvD1.3 with FvE5.2 was analyzed after biotinylation of scFvD1.3 and capture of this species on a sensor chip derivatized with streptavidin. Direct immobilization of scFvD1.3 resulted in sensograms which indicated that less than 30% of the immobilized scFvD1.3 molecules were available for binding (data not shown), implying that coupling of this ligand through its amine groups led to partial inactivation. The biotinylation step greatly improved the quality of sensorgrams, with nearly 70% of the immobilized scFvD1.3 molecules now active. This result is most easily explained by the ability of the spacer arm of the biotinylation reagent (biotinamidocaproate *N*-hydroxysulfosuccinimide ester) to prevent steric hindrance to binding resulting from direct immobilization of the ligand. Depending on the affinities of the mutants tested, FvE5.2 concentrations in equilibrium titrations ranged from 5 nM to 40 μM. As before, significant nonspecific effects on bulk refractive index were observed only for high FvE5.2 concentrations. Typical binding profiles and corresponding Scatchard plots are shown in Figure 3. Controls to establish that the integrity of the streptavidin−biotin interaction and the binding activity of scFvD1.3 were not appreciably affected by repeated washes with HCl were carried out as described above by reinjecting FvE5.2 at several previously tested concentrations. We stress the importance of using a single chain Fv fragment for immobilization since the relatively stringent regeneration conditions could potentially result in the dissociation of V_H and V_L domains, leading to artifactually weak signals.

The K_A for the interaction of wild-type scFvD1.3 with HEL (5.0×10^7 M^{-1}) agrees well with the value determined by fluorescence quenching (6.7×10^7 M^{-1}; Hawkins *et al*., 1992). Association constants for the interaction of HEL with the mutants V_HT30A, V_HW52A, V_HD54A, V_HR99A, and V_H-Y101F (Table 1) are also in reasonable agreement with the values determined by fluorescence quench titration for the dimeric version of the same mutants (Hawkins *et al*., 1994): 5.5×10^7 M^{-1} versus 2.3×10^8 M^{-1}, 2.7×10^7 M^{-1} versus 3.3×10^7 M^{-1}, 1.7×10^7 M^{-1} versus 1.0×10^7 M^{-1}, 5.9×10^7 M^{-1} versus 1.2×10^8 M^{-1}, and 1.0×10^7 M^{-1} versus 4.9×10^6 M^{-1}, respectively. In cases where

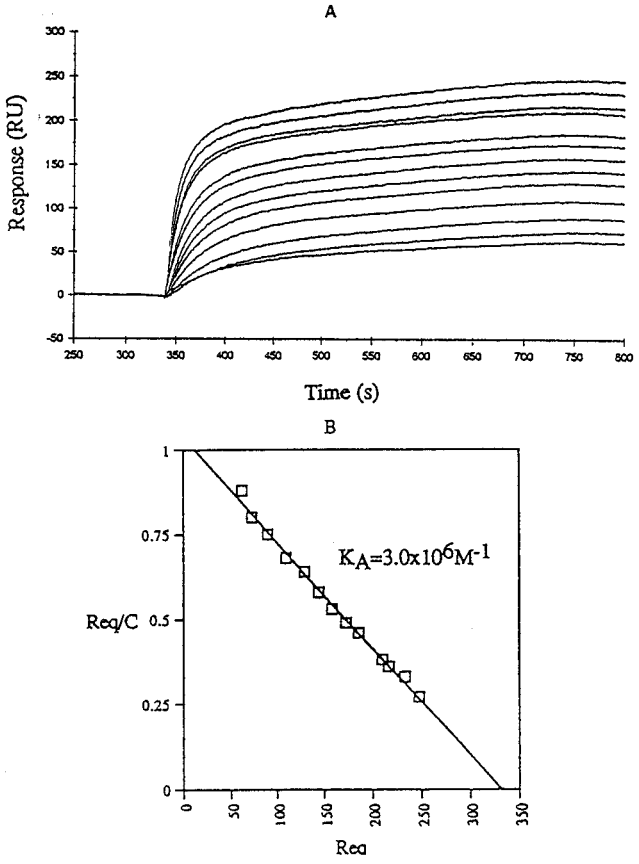

FIGURE 3: (A) Binding of FvE5.2 to the immobilized scFv D1.3 V_LY32A mutant. FvE5.2 was injected at 13 different concentrations ranging from 70 nM to 0.9 μM over a surface on which 500 RU of V_LY32A had been captured on a streptavidin-derivatized chip as described under Materials and Methods. Buffer flow rates were 5 μL/min and report points taken 7 min after each injection. (B) Scatchard plot of the binding of FvE52 to V_LY32A derived from the data in (A) after correction for nonspecific binding. The plot is linear with a correlation coefficient of 0.997. The apparent K_A is 3.0×10^6 M^{-1}. The predicted maximum binding capacity (approximately 330 RU) indicates that about 70% of the immobilized scFvD1.3 molecules are available for binding.

significant discrepancies occur (*e.g.*, V_HT30A), these may be attributed to the presence of the linker peptide, as reported by others (Huston *et al.*, 1988; Denzin & Voss, 1992). Fluorescence quench titration and sedimentation equilibrium measurements were carried out on the scFvD1.3−FvE5.2 reaction as described below to obtain independent checks on the K_A values obtained from BIAcore.

Measurement of D1.3−E5.2 Binding Affinities by Fluorescence Quenching and Sedimentation Equilibrium. While the BIAcore method for determining affinities is rapid and convenient, it requires immobilization of one of the interacting species, a potential source of artifacts. A major advantage of sedimentation equilibrium and fluorescence quench titration is that, in these methods, both interacting species are in solution. Figure 4 shows fluorescence quenching curves for the binding of wild-type scFvD1.3 and a mutant, V_HD58A, to FvE5.2. As shown in Table 1, the calculated K_As (2.7×10^8 M^{-1} and 1.7×10^7 M^{-1}, respectively) agree to within a factor of 3 with the BIAcore values (9.3×10^7 M^{-1} and 6.2×10^6 M^{-1}, respectively). These differences could be due to subtle effects on scFvD1.3 conformation and/or accessibility arising from the immobilization procedure. The K_A value for the V_HW52A mutant obtained by sedimentation equilibrium (9.1×10^4 M^{-1}; Figure 5) is in good agreement with that from BIAcore (8.6×10^4 M^{-1}). We therefore conclude that the BIAcore method is appropriate for affinity measurements in the scFvD1.3−FvE5.2 system over a K_A range of 10^4−10^8 M^{-1}.

Table 1: Association Constants and Relative Free Energy Changes for the Binding of scFvD1.3 Mutants to HEL and FvE5.2[a]

mutant	affinity constant D1.3/E5.2 (M^{-1})	$\Delta\Delta G$ (kcal/mol) D1.3/E5.2	affinity constant D1.3/HEL (M^{-1})	$\Delta\Delta G$ (kcal/mol) D1.3/HEL
wild type	$9.3 \pm 3.3 \times 10^7$ ($2.7 \pm 0.7 \times 10^8$)		$5.0 \pm 0.8 \times 10^7$	
V_LH30A	$5.7 \pm 1.7 \times 10^6$	1.7	$1.2 \pm 0.2 \times 10^7$	0.8
V_LY32A	$3.0 \pm 0.9 \times 10^6$	2.0	$5.2 \pm 0.8 \times 10^6$	1.3
V_LY49A	$5.0 \pm 1.5 \times 10^6$	1.7	$1.3 \pm 0.2 \times 10^7$	0.8
V_LY50A	$2.9 \pm 0.9 \times 10^7$	0.7	$2.6 \pm 0.4 \times 10^7$	0.4
V_LW92A	$5.2 \pm 1.4 \times 10^7$	0.3	$5.0 \pm 0.8 \times 10^5$	2.7
V_LS93A[b]	$1.3 \pm 0.4 \times 10^7$	1.2	$2.8 \pm 0.4 \times 10^7$	0.3
V_HT30A[c]	$2.0 \pm 0.6 \times 10^7$	0.9	$5.5 \pm 0.8 \times 10^7$	0.1
V_HY32A	$4.2 \pm 1.3 \times 10^6$	1.8	$2.3 \pm 0.3 \times 10^7$	0.5
V_HW52A	$8.6 \pm 0.5 \times 10^4$ [9.1×10^4]	4.2	$2.7 \pm 0.4 \times 10^7$	0.4
V_HD54A	$6.7 \pm 2.0 \times 10^4$	4.3	$1.7 \pm 0.3 \times 10^7$	0.6
V_HN56A[c]	$1.3 \pm 0.4 \times 10^7$	1.2	$3.7 \pm 0.6 \times 10^7$	0.2
V_HD58A	$6.2 \pm 1.9 \times 10^6$ ($1.7 \pm 0.3 \times 10^7$)	1.6	$7.1 \pm 1.1 \times 10^7$	−0.2
V_HE98A[c]	$7.9 \pm 2.4 \times 10^4$	4.2	$7.7 \pm 1.1 \times 10^6$	1.1
V_HR99A	$3.9 \pm 1.2 \times 10^6$	1.9	$5.9 \pm 0.9 \times 10^7$	0.1
V_HD100A	$8.3 \pm 2.5 \times 10^5$	2.8	$2.8 \pm 0.4 \times 10^5$	3.1
V_HY101A	ND	>4.0	ND	>4.0
V_HY101F	$3.1 \pm 0.9 \times 10^6$	2.0	$1.0 \pm 0.2 \times 10^7$	1.0

[a] Affinity measurements were carried out by BIAcore as described in Materials and Methods. Numbers in parentheses and brackets are K_A values determined by fluorescence quench titration or sedimentation equilibrium, respectively. Residue numbering is according to Kabat *et al.* (1991). [b] D1.3 residue in contact only with HEL in the crystal structures of the FvD1.3−HEL and FvD1.3−FvE5.2 complexes (Bhat *et al.*, 1994; Fields *et al.*, 1995). [c] D1.3 residues in contact only with E5.2. All other residues are in contact with both HEL and E5.2. Differences in free energy changes are calculated as the differences between the ΔGs of mutant and wild-type reactions ($\Delta\Delta G = \Delta G_{mutant} - \Delta G_{wild\ type}$). For V_HY100A, the $\Delta\Delta G$ values for binding both HEL and E5.2 are estimated at >4 kcal/mol (see Results and Discussion). ND, not determined.

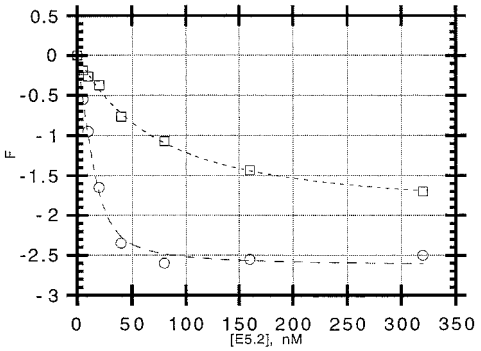

FIGURE 4: Plot of *F* versus concentration of E5.2 showing titration curves for the binding of wild-type scFvD1.3 (○) and the mutant V_HD58A (□). Fitting the curves as described in Materials and Methods leads to a K_A of 2.7×10^8 M^{-1} for the wild type and 1.7×10^7 M^{-1} for the mutant.

Comparison of the Recognition of HEL and E5.2 by D1.3. Crystallographic studies have shown that, of the 18 D1.3 residues that contact E5.2 and the 17 that contact HEL, 13 are in contact with both E5.2 and HEL (Fields *et al.*, 1995; Bhat *et al.*, 1994). To evaluate the relative contribution to binding of D1.3 residues in contact with E5.2 and/or HEL in the crystal structures, a total of 16 single alanine mutants of D1.3 were produced and characterized. The binding

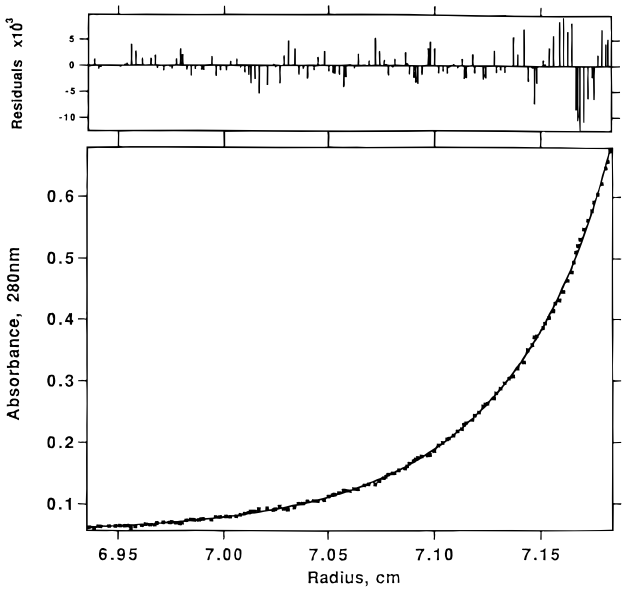

FIGURE 5: Sedimentation equilibrium of an equimolar mixture of the V_HW52A mutant with FvE5.2. Sedimentation was performed as described in Materials and Methods. (Bottom) Absorbance at 280 nm versus distance from the center of rotation in centimeters. (Top) The residuals [A_{280nm} (theoretical) − A_{280nm} (observed)] for the equilibrium between and two components, yielding a K_A of 9.1×10^4 M^{-1}, are small and random.

affinities of wild-type scFvD1.3 and these mutants for FvE5.2 and HEL are shown in Table 1. Because the V_HY101A mutant could not be purified on either HEL or E5.2 affinity columns due to its poor affinity for both species, a more conservative mutant, V_HY101F, was constructed. The K_A of the V_HY101A mutant for both HEL and E5.2 may be estimated at $<8.6 \times 10^4$ M^{-1}, the affinity of the V_HW52A mutant for E5.2, since this latter mutant can be purified by E5.2 chromatography.

Alanine-scanning mutagenesis of D1.3 residues in contact with HEL in the crystal structure of the FvD1.3−HEL complex (Bhat *et al*., 1994) reveals that residues in complementarity-determining region 1 of V_L (V_LCDR1) and V_HCDR3 contribute more to binding than residues in V_LCDR2, V_LCDR3, V_HCDR1, and V_HCDR2 (Table 1). By far the greatest reductions in affinity ($\Delta G_{mutant} - \Delta G_{wild\ type} > 2.5$ kcal/mol) occurred on substituting three residues: V_LW92, V_HD100, and V_HY101. Significant effects (1.0−2.0 kcal/mol) were also seen for substitutions at positions V_LY32 and V_HE98, even though the latter is not involved in direct contacts with HEL. Mutations at nine other contact positions (V_LH30, V_LY49, V_LY50, V_LS93, V_HY32, V_HW52, V_HD54, V_HD58, and V_HR99) had little or no effect (<1.0 kcal/mol). Therefore, the binding of HEL by D1.3 appears to be largely mediated by only 5 of the 14 residues tested. This is similar to findings in the case of human growth hormone binding to its receptor (Cunningham & Wells, 1993; Clackson & Wells, 1995).

For the interaction of D1.3 with E5.2, affinity measurements show that V_HCDR2, V_HCDR3, and V_LCDR1 of D1.3 are more important for binding E5.2 than V_HCDR1, V_LCDR2, and V_LCDR3 (Table 1). Overall, D1.3 V_H residues appear to contribute more to the free energy of binding than V_L residues, since the most destabilizing alanine substitutions (>2.5 kcal/mol) are located in V_HCDR2 (W52A and D54A) and V_HCDR3 (E98A, D100A, and Y101A). Significant

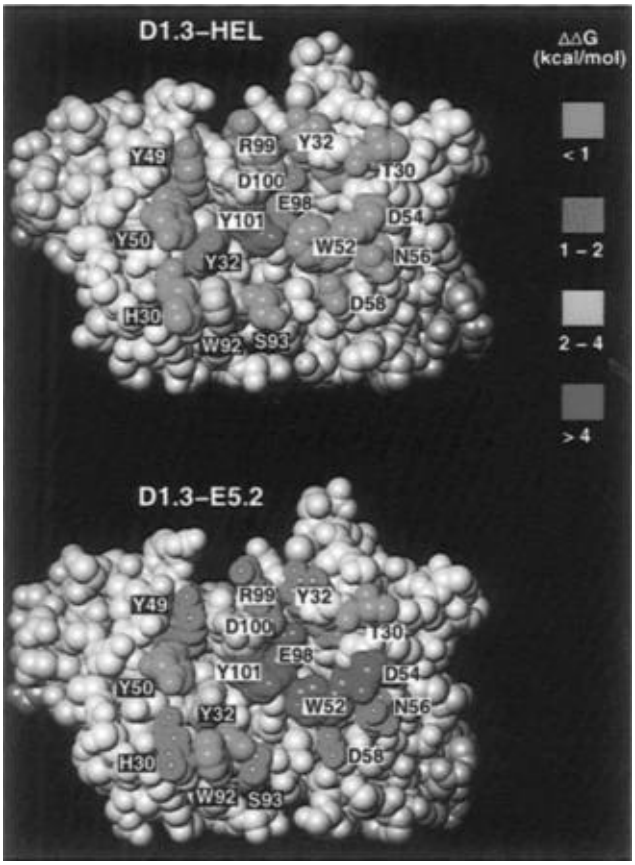

FIGURE 6: Space-filling model of the surface FvD1.3 in contact to HEL and FvE5.2. Residues are color-coded according to the loss of binding free energy upon alanine substitution: red, >4 kcal/mol; yellow, 2−4 kcal/mol; green, 1−2 kcal/mol; blue, <1 kcal/mol.

effects (1.0−2.0 kcal/mol) were also observed for the following contact residues: H30 and Y32 in V_LCDR1, Y49 in V_LCDR2, Y32 in V_HCDR1, N56 and D58 in V_HCDR2, and R99 in V_HCDR3. Mutations at positions V_LY50, V_LW92, and V_HT30 had little or no effect (<1.0 kcal/mol). Thus, of the 15 contact residues tested, 12 make significant contributions to binding E5.2.

It has been proposed that the formation of specific protein−protein complexes is mediated by only a few productive interactions which dominate the energetics of association (Novotny *et al*., 1989; Clackson & Wells, 1995; Nuss *et al*., 1993). In agreement with this notion, our analysis of the scFvD1.3−HEL interaction reveals that only a small subset of the total combining site residues of D1.3 appears to account for a large proportion of the binding energy; most residues (9 of 14) make little or no apparent net contribution (<1.0 kcal/mol). This contrasts with the interaction of D1.3 with E5.2 in which nearly all the contacting residues play a demonstrable role in binding ligand (>1.0 kcal/mol), even though a number of "hot spots" ($\Delta\Delta G$ > 2.5 kcal/mol) are clearly present. Therefore, stabilization of the D1.3−E5.2 complex is achieved by the accumulation of many productive interactions of varying strengths over the entire interface between the two proteins.

Relationship between Structural and Functional Epitopes. Figure 6 shows the functional epitopes of D1.3 involved in binding HEL and E5.2 mapped onto its three-dimensional structure. With the exception of V_LW92, which lies at the periphery, the residues of D1.3 most important for binding

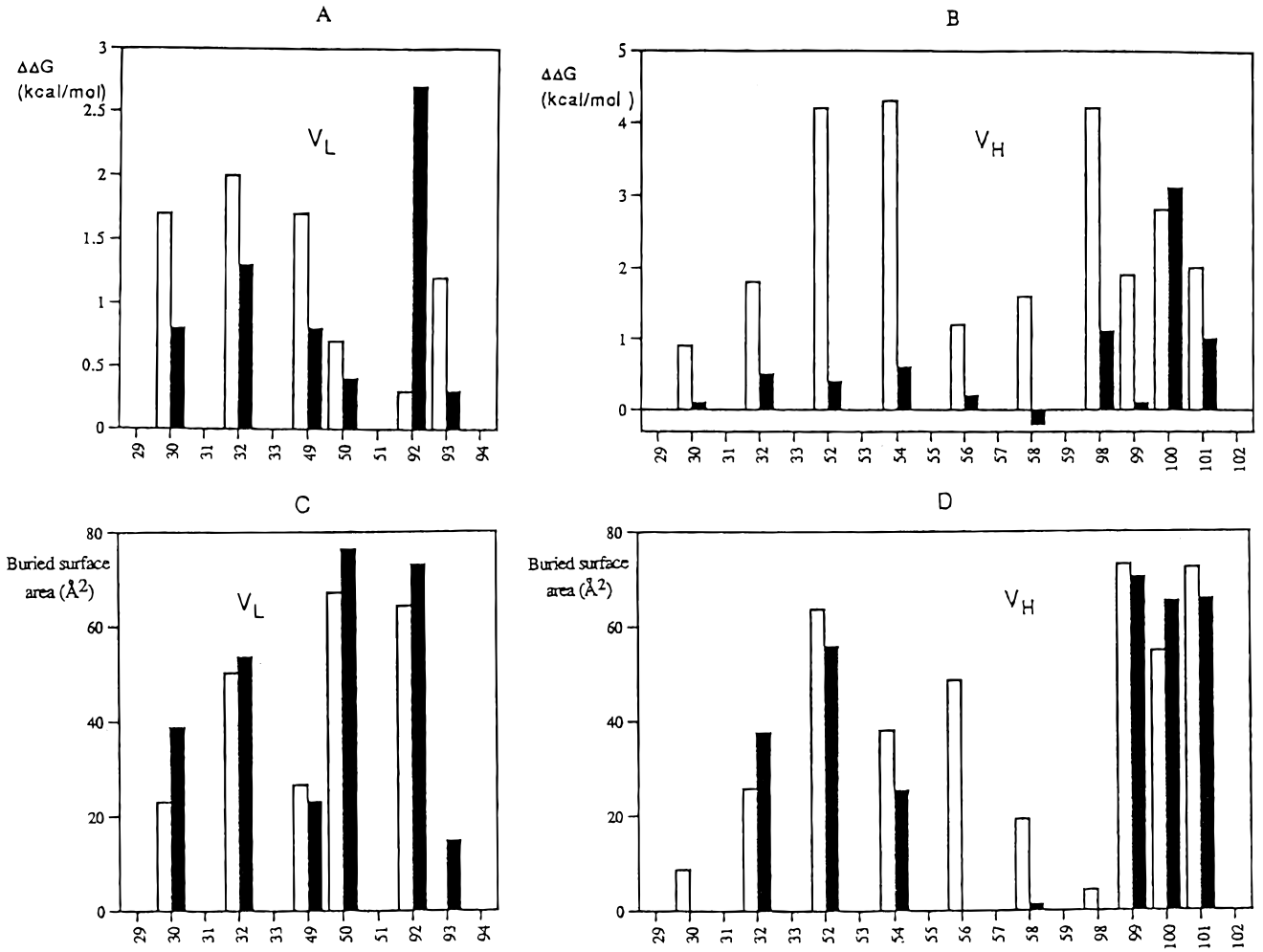

FIGURE 7: (A) Differences in binding free energy changes ($\Delta\Delta G$) between alanine mutants in the V_L domain of scFvD1.3 and the wild-type protein for the interaction with HEL and FvE5.2. (B) Same as (A) for substitutions in the V_H domain. A negative value at position V_H58 indicates a slight increase in apparent affinity for HEL upon alanine substitution. The $\Delta\Delta G$ values for V_HY101 are for the mutant V_HY101F, since the affinity of the corresponding alanine mutant for both HEL and E5.2 was too low to permit purification (see Results and Discussion). (C) Loss of solvent-accessible area (Lee & Richards, 1971) of the side-chain portion of each mutated residue in the V_L domain of scFvD1.3 on forming a complex with FvE5.2 or HEL. (D) Same as (C) for residues in the V_H domain. Bars: (□) E5.2; (■) HEL.

HEL (V_HY101, V_HD100, V_LY32, and V_HE98) are located in a contiguous patch at the center of the combining site (Figure 6). Residues at the periphery make only minor contributions to the binding energy. A similar pattern is observed for the FvD1.3−FvE5.2 complex, with the most important residues (V_LY32, V_HW52, V_HD54, V_HE98, V_HD100, and V_HY101) forming a central band of key contacts. For the most part, however, the hot spots for the two interactions do not overlap. For instance, alanine substitution at position V_LW92 of D1.3 produces a 100-fold decrease in affinity for HEL but does not appreciably affect binding to E5.2 (Table 1). Conversely, the V_HW52A substitution decreases affinity for E5.2 1000-fold but has virtually no effect on binding to HEL. Only substitutions V_HD100A and V_HY101A greatly affect the binding to both HEL and E5.2. Residue V_HY101 contacts HEL and E5.2 mainly through its aromatic side chain while V_HD100 forms an internal salt bridge with V_HR102, which may be important for maintaining the conformation of the V_HCDR3 loop of D1.3 (Bhat *et al*., 1994; Fields *et al*., 1995).

In both complexes, hot spots include hydrophobic (V_LW92, V_HW52, and V_HY101) as well as polar residues (V_HD54, V_HE98, and V_HD100). The data do not show any particular relation between the hydrophobicity of the substituted residue and impact on the binding constant. Both polar and nonpolar residues were also found to play a prominent role in the interaction of human growth hormone with a monoclonal antibody directed against it (Jin *et al*., 1992). These results contrast with those on the binding of growth hormone to its receptor showing that substantial reductions in affinity are only associated with substitution of hydrophonbic residues (Clackson & Wells, 1995). Moreover, the effects of conversion of a number of hydrophobic side chains of D1.3 to alanine are weaker than would be expected if one considers that each buried methylene group contributes −1.0 to −1.5 kcal/mol (Shortle, 1992). For example, substitution of D1.3 residues V_LY50 and V_LW92, whose side chains make a number of van der Waals contacts with residues of E5.2, causes losses in binding energy of only 0.7 and 0.3 kcal/mol, respectively. Similar results are found for mutants V_HY32A and V_HW52A in the case of the D1.3−HEL interaction.

Chothia and Janin (1975) found that a change in buried surface area generally correlated with the free energy of association between two proteins. In Figure 7 we show the apparent contribution of every substituted residue of D1.3

to binding HEL and FvE5.2, as well as the buried surface area of each of these residues upon complex formation. It is clear that buried surface area does not correlate well with the energetic importance of individual residues. In a few cases, this is likely due to secondary effects of the substitution on the conformation of key contact residues. For example, replacement of D1.3 residue V_HE98 greatly reduces affinity for FvE5.2 (4.2 kcal/mol). This residue is mostly buried in the free D1.3 combining site and becomes only slightly more buried when E5.2 binds (Figure 7). Thus, the observed effect on affinity may result from structural perturbations propagated from the alanine mutation to neighboring residues in the functional epitope (V_HY101, V_HW52, and V_HD54). In the majority of cases, however, the results are not so readily explained. Thus, V_HW52 makes a similar number of contacts, over a comparable area, with HEL as it does with E5.2 (Bhat *et al*., 1994; Fields *et al*., 1995), yet the corresponding alanine mutant binds the former 1000-fold more strongly than the latter. A poor correlation between buried surface area and relative contribution to binding was also noted by Cunningham and Wells (1993), who suggested that the role of individual contacts, because of microscopic heterogeneity, could not be predicted from the buried surface area. It may be that, for some residues showing a large buried surface area, the energetic cost of desolvation is comparable to, or exceeds, the energy gained through intermolecular interactions upon formation of the complex, in agreement with the view that burial of hydrophobic residues and release of water molecules are not necessarily the major contributor to the stabilization of protein−protein complexes (Ross & Subramanian, 1981; Bhat *et al*., 1994). Another possibility is that functionally neutral side chains are disordered in the free D1.3 molecule so that a large part of the binding energy is used to "freeze" them in the complex. However, these side chains are well ordered in the 1.8 Å resolution crystal structure of free FvD1.3 (Bhat *et al*., 1990) and, furthermore, do not undergo major conformation changes upon complex formation with HEL or E5.2.

We have shown that a single set of contact residues on D1.3 binds HEL and FvE5.2 in energetically different ways. Thus, although D1.3 recognizes these two proteins in ways that are structurally very similar, this similarity extends only partially to the functional epitopes. This is in agreement with the work of Tulip *et al*. (1994), who found that the anti-neuraminidase antibodies NC10 and NC41 recognize the same protein surface through different key residues. We have also shown that, while the binding of D1.3 to HEL is dominated by only a few residues, the majority of contact residues contribute significantly to binding E5.2. Two broad categories of functional epitopes may be therefore defined: (i) ones in which ligand binding is mediated by a small subset of contact residues and (ii) ones in which the free energy of binding arises from many productive interactions distributed over the entire protein−protein interface.

ACKNOWLEDGMENT

We are grateful to Michael Robinson (Pharmacia Biosensor) and Emilio Malchiodi (CONICET, Argentina) for advice on affinity measurements. We thank Barry Fields for discussions and help in preparing the figures and Marina Lebedeva and Lukas Leder for critical reading of the manuscript.

REFERENCES

Bhat, T. N., Bentley, G. A., Fischman, T. O., Boulot, G., & Poljak, R. J. (1990) *Nature 347*, 483−485.
Bhat, T. N., Bentley, G. A., Boulot, G., Greene, M. I., Tello, D., Dall'Acqua, W., Souchon, S., Schwartz, F. P., Mariuzza, R. A., & Poljak, R. J. (1994) *Proc. Natl. Acad. Sci. U.S.A. 91*, 1089−1093.
Braden, B. C., & Poljak, R. J. (1995) *FASEB J. 9*, 9−16.
Brooks, I. S., Soneson, K. K., & Hensley, P. (1993) *Biophys. J. 64*, A244.
Brooks, I., Wetzel, R., Chan, W., Lee, G., Watts, D. G., Soneson, K. K., & Hensley, P. (1994) in *Modern Analytical Ultracentrifugation. Acquisition and Interpretation of Data for Biological and Synthetic Polymer Systems* (Schuster, T. M., & Laue, T. M., Eds.) pp 15−36, Birkhauser, Boston.
Chothia, C., & Janin, J. (1975) *Nature 256*, 705−708.
Clackson, T., & Wells, J. A. (1995) *Science 267*, 383−386.
Cunningham, B. C., & Wells, J. A. (1993) *J. Mol. Biol. 234*, 554−563.
Davies, D. R., & Cohen, G. H. (1996) *Proc. Natl. Acad. Sci. U.S.A. 93*, 7−12.
Davies, D. R., Padlan, E., & Sheriff, S. (1990) *Annu. Rev. Biochem. 59*, 439−473.
Denzin, L. K., & Voss, E. W. (1992) *J. Biol. Chem. 267*, 8925−8931.
Fersht, A. R. (1988) *Biochemistry 27*, 1577−1580.
Fields, B. A., Goldbaum, F. A., Ysern, X., Poljak, R. J., & Mariuzza, R. A. (1995) *Nature 374*, 739−742.
Foote, J., & Winter, G. (1992) *J. Mol. Biol. 224*, 487−499.
Goldbaum, F. A., Fields, B. A., Cauerhff, A., Ysern, X., Houdusse, A., Eisele, J. L., Poljak, R. J., & Mariuzza, R. A. (1994) *J. Mol. Biol. 241*, 739−743.
Goldbaum, F. A., Schwartz, F. P., Eisenstein, E., Cauerhff, A., Mariuzza, R. A., & Poljak, R. J. (1996) *J. Mol. Recogn.* (in press).
Granzow, R., & Reed, R. (1992) *Bio/Technology 10*, 390−393.
Hawkins, R. E., Russell, S. J., & Winter, G. (1992) *J. Mol. Biol. 226*, 889−896.
Hawkins, R. E., Russell, S. J., Baier, M., & Winter, G. (1993) *J. Mol. Biol. 234*, 958−964.
Hochuli, E., Bannwarth, W., Dobeli, H., Gentz, R., & Stuber, D. (1988) *Bio/Technology 6*, 1321−1325.
Huston, J. S., Levinson, D., Mudgett-Hunter, M., Tai, M. S., Novotny, J., Margolies, M. N., Ridge, R. J., Bruccoleri, R. E., Haber, E., Crea, R., & Oppermann, H. (1988) *Proc. Natl. Acad. Sci. U.S.A. 85*, 5879−5883.
Ito, W., Iba, Y., & Kurosawa, Y. (1993) *J. Biol. Chem. 268*, 16638−16647.
Janin, J., & Chothia, C. (1990) *J. Biol. Chem. 265*, 16027−16030.
Jin, L., Fendly, B. M., & Wells, J. A. (1992) *J. Mol. Biol. 226*, 851−865.
Johnson, M. L., & Fraser, S. G. (1985) *Methods Enzymol. 117*, 301−342.
Johnson, M. L., Correia, J. J., Yphantis, D. A., & Halvorson, H. R. (1981) *Biophys. J. 36*, 575−588.
Johnsson, B., Lofas, S., & Lindquist, G. (1991) *Anal. Biochem. 198*, 268−277.
Kabat, E. A., Wu, T. T., Perry, H. M., Gottesman, K. S., & Foeller (1991) *Sequences of Proteins of Immunological Interest*, U.S. Public Health Service, National Institutes of Health, Washington, DC.
Karlsson, R., Michaelsson, A., & Mattson, L. (1991) *J. Immunol. Methods 145*, 229−240.
Kelley, R. F., & O'Connell, M. P. (1993) *Biochemistry 32*, 6828−6835.
Kornblatt, J., Kornblatt, M. J., Hui Bon Hoa, G., & Mauk, A. G. (1993) *Biophys. J. 65*, 1059−1065.
Kunkel, T. A., Roberts, J. D., & Zakour, R. A. (1987) *Methods Enzymol. 154*, 367−382.
Lee, B. K., & Richards, F. M. (1971) *J. Mol. Biol. 55*, 379.
Malchiodi, E. L., Eisenstein, E., Fields, B. A., Ohlendorf, D. H., Schlievert, P. M., Karjalainen, K., & Mariuzza, R. A. (1995) *J. Exp. Med. 182*, 1833−1845.

Mariuzza, R. A., & Poljak, R. J. (1993) *Curr. Opin. Immunol. 5*, 50−55.
Mariuzza, R. A., Jankovic, D. Lj., Boulot, G., Amit, A. G., Saludjian, P., Le Guern, A., Mazie, J.-C., & Poljak, R. J. (1984) *J. Mol. Biol. 170*, 1055−1058.
McCafferty, J., Griffiths, A. D., Winter, G., & Chiswell, D. J. (1990) *Nature 348*, 552−554.
Novotny, J., Bruccoleri, R. E., & Saul, F. A. (1989) *Biochemistry 28*, 4735−4749.
Nuss, J. M., Bossart, P. J., & Air, G. M. (1993) *Proteins*: *Struct., Funct., Genet. 15*, 121−132.
Raghavan, M., Chen, M. Y., Gastinel, L. N., & Bjorkman, P. J. (1994) *Immunity 1*, 303−315.
Roark, D. E. (1976) *Biophys. Chem. 5*, 185−196.
Ross, P. D., & Subramanian, S. (1981) *Biochemistry 20*, 3096−3102.
Ruther, U., Koenen, M., Otto, K., & Muller-Hill, B. (1981) *Nucleic Acids Res. 9*, 4087−4098.
Sanger, F., Nicklen, S., & Coulson, A. R. (1977) *Proc. Natl. Acad. Sci. U.S.A. 74*, 5463−5467.
Scatchard, G. (1949) *Ann. N.Y. Acad. Sci. 51*, 660.
Seth, A., Stern, L. J., Ottenhoff, T. H. M., Engel, I., Owen, M. J., Lamb, J. R., Klausner, R. J., & Wiley, D. C. (1994) *Nature 369*, 324−327.
Shortle, D. (1992) *Q. Rev. Biophys. 25*, 205−250.
Tulip, W. R., Varghese, J. N., Webster, R. G., Laver, W. G., & Colman, P. M. (1992) *J. Mol. Biol. 227*, 149−159.
Tulip, W. R., Harley, V. R., Webster, R. G., & Novotny, J. (1994) *Biochemistry 33*, 7986−7997.
van der Merwe, P. A., Brown, M. H., Davis, S. J., & Barclay, A. N. (1993) *EMBO J. 12*, 4945−4954.
van der Merwe, P. A., Barclay, A. N., Mason, D. W., Davies, E. A., Morgan, B. P., Tone, M., Krishnam, A. K. C., Ianelli, C., & Davis, S. J. (1994) *Biochemistry 33*, 10149−10160.
Ward, E. S. (1992) *J. Mol. Biol. 224*, 885−888.
Ward, E. S., Gussow, D., Griffiths, A. D., Jones, P. T., & Winter, G. (1989) *Nature 341*, 544−546.
Ward, L. D. (1985) *Methods enzymol. 117*, 400−414.
Webster, D. M., Henry, A. H., & Rees, A. R. (1994) *Curr. Opin. Struct. Biol. 4*, 123−129.
Wells, J. A. (1991) *Methods Enzymol. 202*, 390−411.
Wilson, L. A., & Stanfield, R. L. (1993) *Curr. Opin. Struct. Biol. 3*, 113−118.
Ysern, X., Fields, B. A., Bhat, T. N., Goldbaum, F. A., Dall'Acqua, W., Schwartz, F. P., Poljak, R. J., & Mariuzza, R. A. (1994) *J. Mol. Biol. 238*, 496−500.

BI960819I